Liquid Crystals

Physical properties of laterally fluorinated isothiocyanato phenyl-tolane liquid crystals

S. Gauza [a]; A. Parish [a]; S. -T. Wu [a]; A. Spadło [b]; R. Dabrowski [b]
[a] College of Optics and Photonics, University of Central Florida, Orlando, Florida 32816, USA
[b] Institute of Chemistry, Military University of Technology, 00-908 Warsaw, Poland

PLEASE SCROLL DOWN FOR ARTICLE

Taylor & Francis
Taylor & Francis Group

Physical properties of laterally fluorinated isothiocyanato phenyl-tolane liquid crystals

S. Gauza[a]*, A. Parish[a], S.-T. Wu[a], A. Spadło[b] and R. Dabrowski[b]

[a]*College of Optics and Photonics, University of Central Florida, Orlando, Florida 32816, USA;* [b]*Institute of Chemistry, Military University of Technology, 00-908 Warsaw, Poland*

We have designed, synthesised and evaluated the physical properties of some high-birefringence (Δn) isothiocyanato phenyl-tolane liquid crystals. These compounds exhibit $\Delta n \sim 0.48$–0.52 at room temperature and wavelength $\lambda = 633$ nm. Laterally substituted fluorine atoms eliminate smectic phases and lower the melting temperature. The moderate melting temperature and very high clearing temperature make those compounds attractive for eutectic mixture formulation.

Keywords: high birefringence; isothiocyanato phenyl-tolanes; eutectic mixtures

1. Introduction

High-birefringence (Δn) liquid crystals (LCs) play an important role in laser beam steering, tuneable-focus lens, reflective display, cholesteric LC laser, infrared dynamic scene projector and telecom variable optical attenuator applications (1). Fast response time is particularly important for colour-sequential liquid crystal displays (LCDs) using a blinking backlight (2) or primary colour (RGB) light-emitting diodes (LEDs) (3, 4). For these devices, high Δn improves response time through cell gap (d) reduction. This advantage is especially important for laser beam steering (5) and variable optical attenuators (6) since these devices are normally operated in the near-infrared region ($\lambda = 1.55 \mu m$). In the long wavelength region, the LC optical path difference ($d\Delta n$) should increase in order to achieve the required phase change, which depends on the specific LC alignment. High birefringence helps to reduce the cell gap in order to maintain fast response time (7).

To achieve high birefringence, linearly conjugated molecules are the preferred candidates (8). Conjugation length can be extended by multiple bonds or unsaturated rings in the rigid core. The three most important problems associated with highly conjugated LC compounds are high melting temperature, increased viscosity, and reduced UV stability (9). Eutectic mixtures can be used to overcome high melting temperature. The increased viscosity is inherent to all the highly conjugated compounds. Isothiocyanato (NCS) compounds are less viscous than the cyano (CN) ones, but the consequence of utilising NCS compounds is that they tend to exhibit smectic phases (10). Due to increased absorption at UV wavelengths, these high-birefringence compounds need to be protected from direct UV exposure but in general are suitable for infrared applications (11).

Several high-birefringence molecular structures, such as cyano and NCS tolanes (12, 13), diphenyl-diacetylene (14, 15), bistolane (16, 17), naphthalene tolanes (18) and thiophenyl-diacetylene (19–21) have been studied. Recently, several phenyl-tolane compounds were synthesised and their properties investigated (22–24). The birefringence of these compounds is in the 0.4–0.6 range.

In this paper, we present several isothiocyanato phenyl-tolane compounds with extrapolated birefringence ~ 0.48–0.52 at $\lambda = 633$ nm and $T = 23°C$. To lower the melting temperature, we tried different lateral fluorinations.

2. Experimental

Several measurement techniques were used to measure the physical properties of the single compounds and mixtures. Differential scanning calorimetry (DSC, TA Instrument Model Q-100) was used to determine the phase transition temperatures. Results were obtained from 3–6 mg samples in the heating and cooling cycles at a rate of $2°C \, min^{-1}$. The electro-optical properties of the LC compounds and mixtures were measured using $5 \mu m$ homogenous cells with ITO (indium–tin oxide) electrodes coated in the inner sides of the glass substrates. A thin polyimide layer was over-coated on ITO and buffed in anti-parallel directions to produce a small pretilt angle ($\sim 2°$). A linearly polarised He–Ne laser with $\lambda = 633$ nm was used as the light source for the electro-optical measurements. Experimental setup and measurement technique were the same as those reported elsewhere (25).

---

*Corresponding author. Email: sgauza@mail.ucf.edu
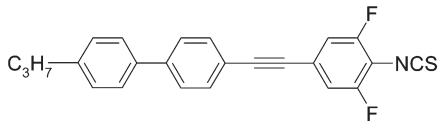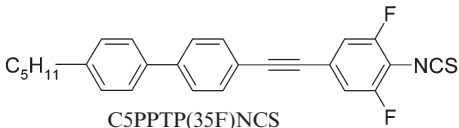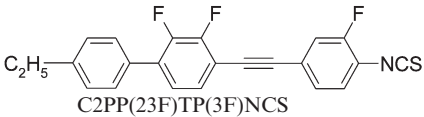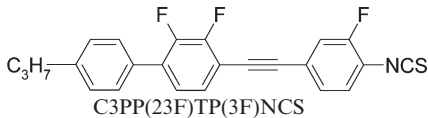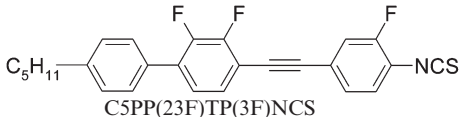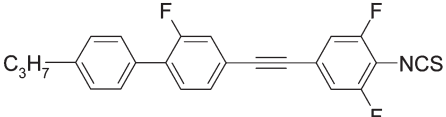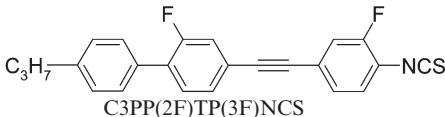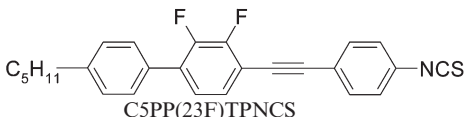
3. Results and discussion

Mesomorphic properties

Table 1 lists the molecular structures and phase transition temperatures of eight isothiocyanato phenyl-tolane LCs investigated. Different lateral fluorination was introduced into a rigid core of a phenyl-tolane in order to lower the melting point of the single compounds. Additional advantages of multiple fluorinations are to suppress or completely eliminate the smectic (Sm) phase from the meso-morphic sequence of such compounds, and to lower the phase transition temperatures. Although there is a substantial improvement in mesomorphic properties over non-fluorinated phenyl-tolane isothiocyanates, our investigation shows that even with lateral substitution(s), the melting temperatures of these compounds are still relatively high. The difluoro-substituted isothiocyanato-tolane compounds, **1** and **2**, exhibit a wide nematic range with clearing point temperatures exceeding 200°C.

The propyl homologue (Compound **1**) exhibits a melting transition at 122°C, which is relatively high. The pentyl homologue (Compound **2**) shows a much lower melting point temperature of 55°C, but its smectic to nematic transition occurs at 119°C. The fusion enthalpy (ΔH) is significantly different for the C3 and C5 homologues. Compound **1**, having a

Table 1. Molecular structures and phase transition temperatures of eight phenyl-tolane isothiocyanates.

ID No.	Structure	Phase transition temperatures /°C	ΔH (Cr–N) /kcal mol^{-1}
1	C3PPTP(35F)NCS	Cr 122.0 N 233.6 I	6.263
2	C5PPTP(35F)NCS	Cr 55.0 Sm 119.0 N 208.5 I	3.770
3	C2PP(23F)TP(3F)NCS	Cr 73.7 N 223.3 I	5.452
4	C3PP(23F)TP(3F)NCS	Cr 82.2 Sm 89.2 N 240.5 I	5.814
5	C5PP(23F)TP(3F)NCS	Cr 53.5 Sm 135.0 N 218.0 I	3.359
6	C3PP(2F)TP(35F)NCS	Cr 110.6 N 204.1 I	7.738
7	C3PP(2F)TP(3F)NCS	Cr 124.0 N 225.9 I	7.234
8	C5PP(23F)TPNCS	Cr 75.0 Sm 152 N 233 I	6.550

shorter alkyl chain, has $\Delta H \sim 6.3\,\mathrm{kcal\,mol}^{-1}$, which is about twice as high as that of Compound **2**, which has a five-carbon alkyl chain. A different lateral fluorination scheme was utilised for the second homologue series (Compounds **3**, **4** and **5**) investigated. This triple fluorination scheme has a fluorine substitution in the second and third positions of the middle phenyl ring, whereas the last phenyl ring has a single fluorine substitution at the position adjacent to the NCS terminal group. The measured melting point temperature for these compounds is significantly lower than that observed for difluorinated Compounds **1** and **2**, but only the ethyl homologue does not exhibit a smectic phase. The pentyl homologue in this series shows an exceptionally low fusion enthalpy $\Delta H \sim 3.4\,\mathrm{kcal\,mol}^{-1}$. Although the melting temperatures for Compounds **3**, **4**, and **5** are relatively low, the smectic phase present in the propyl and pentyl homologues decreases their attractiveness. The positions of the laterally substituted fluorine in Compound **6** are different from the trifluorinated phenyl-tolanes already discussed. The middle phenyl ring has a fluoro group at the second position while the last phenyl link with the terminal NCS group is fluorinated in the $(3,\ 5)$ positions, similar to Compounds **1** and **2**. Comparing the propyl homologues (Compounds **1** and **6**) shows that additional fluorine substituted at the middle ring slightly decreases melting temperature. Comparing the melting temperatures of Compounds **1** and **7** as well as **2** and **8** shows that fluorination of the phenyl ring adjacent to the NCS group results in the best mesomorphic properties of the difluorinated series considered.

Electro-optical properties

Most device applications are performed at room temperature ($\sim23^\circ$C). Thus, the physical properties of these high-melting compounds at room temperature are of interest. Two methods are commonly employed to extrapolate the electro-optical properties of these single compounds at room temperature: (1) guest–host system and (2) fitting extrapolation from elevated temperature results. In the first method, about $10\,\mathrm{wt\,\%}$ of the guest compound to be investigated is dissolved in a room temperature LC host mixture. By knowing the birefringence of the host mixture, the Δn of the guest compound at room temperature can be estimated according to the following equation:

$$(\Delta n)_{gh} = x(\Delta n)_g + (1-x)(\Delta n)_h, \qquad (1)$$

where gh, g and h denote the birefringence of the guest–host system, guest compound and host mixture,

respectively. In the second method, we measure the properties of the compound at several temperatures in its nematic phase, fit the experimental data with models and finally extrapolate the results to room temperature. In this study, we focused on the birefringence (Δn), viscoelastic coefficient (γ_1/K_{11}) and figure-of-merit which is defined as (*26*):

$$\mathrm{FoM} = K_{11}\Delta n^2/\gamma_1, \qquad (2)$$

where K_{11} is the elastic constant and γ_1 the rotational viscosity. The temperature-dependent birefringence of an LC can be described as follows:

$$\Delta n = \Delta n_o(1 - T/T_c)^\beta, \qquad (3)$$

where the fitting parameters are Δn_o, the birefringence at $T=0\,$K, β is a material constant and T_c is the clearing temperature of the LC. By fitting the experimental data using Equation (3), we can obtain Δn_o and β. Once these two parameters are determined, the birefringence of the LC at room temperature can be extrapolated as well as at every other temperature within the nematic phase of an investigated LC compound or mixture. Similarly, we can fit FoM with following Equation (*26*):

$$\mathrm{FoM} = \alpha(\Delta n)^2\left(1 - \frac{T}{T_c}\right)^{3\beta}\exp\left(\frac{-E}{\kappa T}\right), \qquad (4)$$

where a is a fitting parameter. The extrapolated viscoelastic coefficient at room temperature can be calculated from Equation (2). In this study, we chose to use the fitting and extrapolation method instead of guest–host method to determine compound properties at room temperature.

Figure 1 shows the temperature-dependent birefringence of selected di- and trifluorinated phenyl-tolanes based on the fittings of experimental data using Equation (3). Among presented compounds, the difluorinated compound **1** has the highest birefringence (its extrapolated $\Delta n \sim 0.52$ at 20°C), whereas the least attractive is compound **6** ($\Delta n \sim 0.48$) based on this comparison.

From Equations (3) and (4), the birefringence of an LC strongly depends on the clearing point temperature. Compounds with higher clearing point temperatures are more likely to show higher birefringence at low temperatures if the core structures are similar. If compounds of equal alkyl chain length are compared, it is evident that fewer lateral fluorine substitutions preserve higher birefringence. The comparison of two differently trifluorinated Compounds, **4** and **6**, shows noticeable difference in
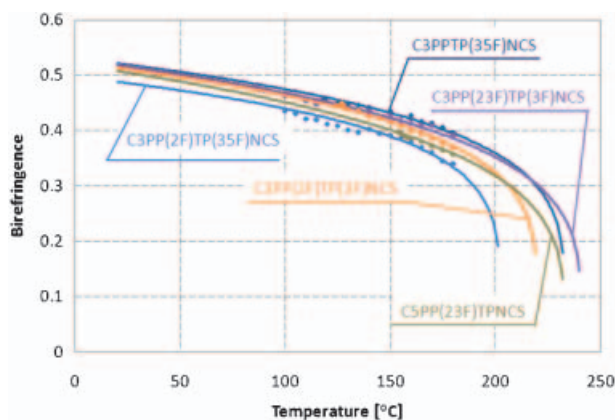
Figure 1. Temperature-dependent birefringence of short alkyl chain NCS-phenyl-tolanes.

birefringence if extrapolated to 20°C, respectively, 0.52 and 0.48. It suggests that difluorination of the middle ring and single fluorine substitution adjacent to the terminal NCS group is more favourable than single fluorination of the middle ring (in the position 2) of the phenyl-tolane unit with difluorinated phenyl ring with NCS group. Introducing a longer alkyl chain slightly decreases the birefringence because of the lower molecular packing density which likely affects the thermal stability of the nematic phase and lowers the clearing temperature for the investigated homologue series. This effect is shown in Figure 2 through the comparison of Compounds **3**, **4** and **5**, which differ only by the length of an alkyl chain. Birefringence extrapolated to 20°C decreases as the alkyl chain length increases, respectively 0.52 for Compounds **3** and **4**, and 0.50 for Compound **5**.

By measuring the free relaxation time of a homogeneous cell, we are able to calculate the viscoelastic coefficient of the LC Compounds (27) expressed by the ratio of the rotational viscosity and splay elastic constant, γ_1/K_{11}. The results are depicted
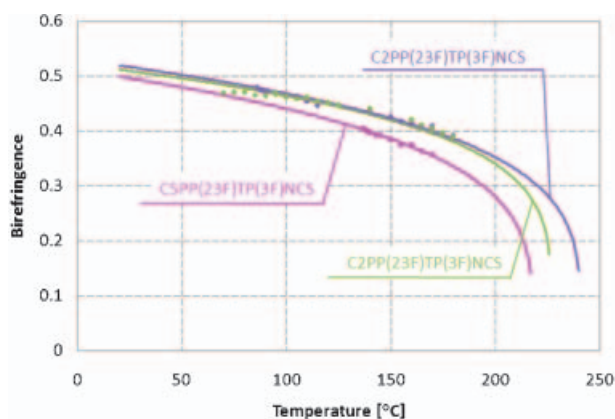
in Figure 3. We found that Compounds **6** and **7** show the highest viscoelastic coefficient among the investigated LC structures. It is interesting to note that Compound **7** has only two lateral fluorine atoms but its viscoelastic coefficient is high. It seems that despite the total number of lateral fluorines, if the middle ring has a fluoro substitution in position 2 it may lead to a large viscoelastic coefficient. Compound **4**, a trifluorinated structure with difluorinated middle phenyl ring in the molecular rigid core, exhibits a moderate viscoelastic coefficient. The value of γ_1/K_{11} we measured for difluorinated Compound **8** was almost the lowest among the investigated compounds. Even with a long, five-carbon alkyl chain, Compound **8** shows just slightly higher viscoelastic coefficient than Compound **1**, especially at the extrapolated temperature range. Considering the difluorinated compounds with different positions of lateral fluorination, we observe the following sequence of γ_1/K_{11} values:

Compound **1** < Compound **8** < Compound **7**.

Such a comparison suggests that, from the viewpoint of viscoelastic coefficient, lateral difluorination within adjacent positions of the same phenyl ring is more attractive than monofluorination of different phenyl rings within the same rigid core of a tolane part of investigated molecules. At this point we have to clarify that our short conclusions are solely based on the choice of the structures listed in Table 1. Further structural modifications are possible upon further synthesis of larger variety of fluorinated phenyl-tolane cores.

When the γ_1/K_{11} coefficient is compared for Compounds **3**, **4** and **5**, which share a common rigid core, the pentyl homologue (Compound **5**) exhibits the lowest value. This result is similar to the comparison of double-fluorinated compounds, for

Figure 2. Temperature-dependent birefringence of NCS-phenyl-tolanes with different lengths of alkyl chain.
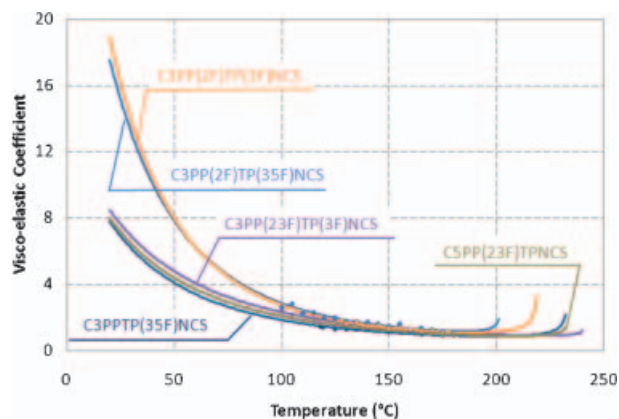

Figure 3. Temperature-dependent viscoelastic coefficient of short alkyl chain NCS-phenyl-tolanes.
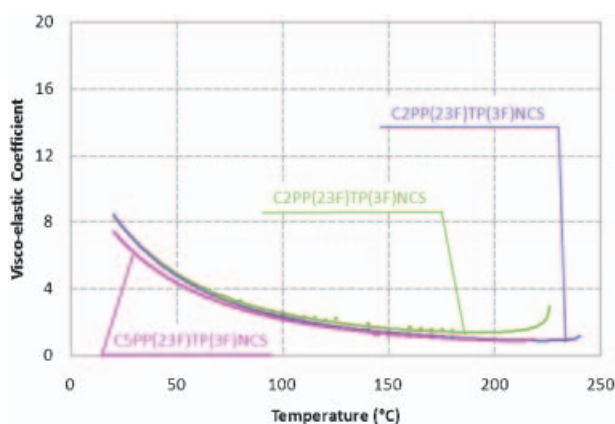
Figure 4. Temperature-dependent viscoelastic coefficient of NCS-phenyl-tolanes with different lengths of alkyl chain.

which the pentyl homologue (Compound **8**) also demonstrates the lowest γ_1/K_{11} value. The ethyl homologue (Compound **3**) exhibits a slightly higher viscoelastic coefficient than the other two homologues with a shorter alkyl chain length, which we assign into higher molecular packaging density as the flexible alkyl chain gets shorter. Figure 4 compares the viscoelastic coefficients for Compounds **3**, **4** and **5**.

Here, we would like to focus on the Figure-of-Merit (FoM) as the most important comparison, taking birefringence and viscoelastic coefficient into consideration according to Equation (2). Figure 5 shows the temperature-dependent FoM of di- and trifluorinated phenyl-tolanes.

Among all the compounds investigated, the difluorinated Compound **1** shows the highest FoM, which is $180\,\mu m^2\,s^{-1}$ at 160–$170°C$. Conversely, the trifluorinated Compound **6** exhibits the lowest FoM, barely reaching $100\,\mu m^2\,s^{-1}$ at its optimal temperature. The reason that Compound **6** has the lowest FoM is because of its lowest birefringence and very high viscoelastic coefficient. The decreased
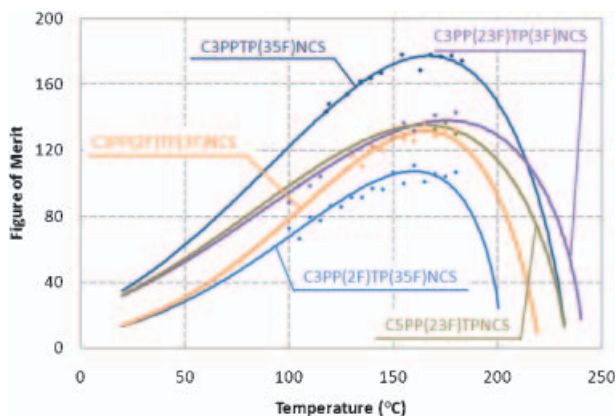
birefringence of Compound **6** is significantly affected by its low clearing temperature.

An observation, made on comparison of compounds **4** and **6**, which differ only in the positions of lateral fluorination, shows the importance of the position(s) at which fluorine is substituted (see Figures 5 and 6). The measured mesomorphic properties and electro-optical performance are significantly different for these two different patterns of trifluorination.

Compound **6**, with two fluoro substitutions adjacent to the NCS terminal group, has a relatively high melting point and low clearing point such that the nematic range is relatively narrow, as compared to Compound **4**. The low T_c of Compound **6** negatively affects its birefringence and, moreover, its viscoelastic coefficient is relatively high. As a result, its FoM is low. In contrast, Compound **4** demonstrates a respectable FoM of $140\,\mu m^2\,s^{-1}$ at the optimal temperature, which is slightly higher than that of the difluorinated Compounds **7** and **8**. The high melting point of compound **7** and stable smectic phase of Compound **8** up to $152°C$ make these compounds less attractive for mixture formulation than the trifluorinated Compounds **3** and **4**.

4. Conclusion

We have developed eight laterally fluorinated phenyl-tolane isothiocyanates and evaluated their mesomorphic and electro-optical properties. Multiple fluorinations lower the melting temperature of the single compounds but the trade-off is the increased viscosity. Introduction of lateral fluorine also affects the interactions between neighbouring molecules as transverse dipole moments are introduced, especially when single fluorination takes place in the middle phenyl ring of the rigid core. A certain compromise needs to be made between high FoM and low melting
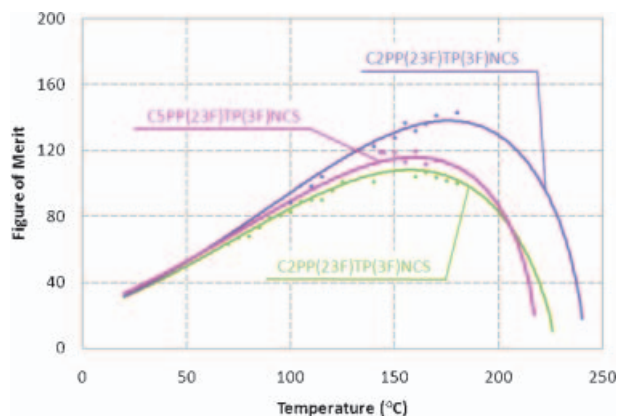

Figure 5. Temperature-dependent FoM of short alkyl chain NCS-phenyl-tolanes.

Figure 6. Temperature-dependent FoM of NCS-phenyl-tolanes with different lengths of alkyl chain.

488   S. Gauza et al.

temperature of the compounds. We found that having the middle phenyl difluorinated, without additional fluorination on the phenyl ring linked with terminal NCS group decreases visco-elastic coefficient. It is at present unclear whether this situation is similar to the one observed for laterally fluorinated dialkyl terphenyl compounds (28). From the mixture formulation standpoint, the most favourable among discussed fluorination patterns of the phenyl-tolane core with NCS terminal group are presented by Compounds **1** and **3**. Further synthesis needs to be performed in order to make extended and more detailed comparison of possible additional patterns. Our overall conclusion is that the presented fluorinated phenyl-tolane isothiocyanates show high FoM and are particularly attractive for long-wavelength applications, such as laser beam steering and variable optical attenuators, where high birefringence allows a thin cell gap to be used for achieving a fast response time. The UV stability of these compounds is not a concern for IR applications.

Acknowledgments

References

(1) Wu S.T.; Yang D.K. *Reflective Liquid Crystal Displays*; Wiley: New York, 2001.
(2) Nishiyama K.; Okita M.; Kawaguchi S.; Teranishi K.; Takamatsu R. *SID Tech. Dig.* **2005**, *36*, 132–135.
(3) Hsieh H.S.; Chou C.H.; Li W.Y. *Proceedings of the International Display Manufacturing Conference; SID,* **2005**, *622–625*.
(4) Harbers G.; Hoelen C. *SID Tech. Dig.* **2001**, *32*, 702–705.
(5) McManamon P.F.; Dorschner T.A.; Corkum D.L.; Friedman L.; Hobbs D.S.; Holz M.; Liberman S.; Nguyen H.Q.; Resler D.P.; Sharp R.C., *et al. Proc. IEEE* **1996**, *84*, 268–298.
(6) Liang X.; Lu Y.Q.; Wu Y.H.; Wang H.; Wu S.T. *Jap. J. Appl. Phys., Pt. 1* **2005**, *44*, 1292–1295.
(7) Wu S.T.; Efron U. *Appl. Phys. Lett.* **1986**, *48*, 624–626.
(8) Wu S.T. *Phys. Rev. A* **1986**, *33*, 1270–1274.
(9) Gauza S.; Wen C.H.; Wu S.T.; Janarthanan N.; Hsu C.S. *Jap. J. Appl. Phys., Pt. 1* **2004**, *43*, 7634–7638.
(10) Spadło A.; Dąbrowski R.; Filipowicz M.; Stolarz Z.; Przedmojski J.; Gauza S.; Fan Y.H.; Wu S.T. *Liq. Cryst.* **2003**, *30*, 191–198.
(11) Wu S.T. *Opt. Engng* **1987**, *26*, 120–128.
(12) Wu S.T.; Cox R.J. *J. Appl. Phys.* **1988**, *64*, 821–826.
(13) Gauza S.; Wang H.; Wen C.H.; Wu S.T.; Seed A.; Dabrowski R. *Jap. J. Appl. Phys., Pt. 1* **2003**, *42*, 3463–3466.
(14) Wu S.T.; Margerum J.D.; Meng B.; Dalton L.R.; Hsu C.S.; Lung S.H. *Appl. Phys. Lett.* **1992**, *61*, 630–632.
(15) Wu S.T.; Neubert M.; Keast S.S.; Abdallah D.G.; Lee S.N.; Walsh M.E.; Dorschner T.A. *Appl. Phys. Lett.* **2000**, *77*, 957–959.
(16) Wu S.T.; Hsu C.S.; Shyu K.F. *Appl. Phys. Lett.* **1999**, *74*, 344–346.
(17) Wu S.T.; Hsu C.S.; Chuang Y.Y.; Cheng H.B. *Jap. J. Appl. Phys., Pt. 2* **2000**, *39*, L38–L41.
(18) Seed A.J.; Toyne K.J.; Goodby J.W.; Hird M. *J. Mater. Chem.* **2000**, *10*, 2069–2080.
(19) Sekine C.; Konya N.; Minai M.; Fujisawa K. *Liq. Cryst.* **2001**, *28*, 1361–1367.
(20) Sekine C.; Ishitobi M.; Iwakura K.; Minai M.; Fujisawa K. *Liq. Cryst.* **2002**, *29*, 355–367.
(21) Sekine C.; Konya N.; Minai M.; Fujisawa K. *Liq. Cryst.* **2001**, *28*, 1495–1503.
(22) Catanescu O.; Chien L.C. *Liq. Cryst.* **2006**, *33*, 115–120.
(23) Gauza S.; Wu S.T.; Spadlo A.; Dabrowski R. *J. Display Technol.* **2006**, *2*, 247–253.
(24) Gauza S.; Wen C.H.; Wu B.; Wu S.T.; Spadlo A.; Dabrowski R. *Liq. Cryst.* **2006**, *33*, 705–710.
(25) Wu S.T.; Efron U.; Hess L.D. *Appl. Opt.* **1984**, *23*, 3911–3915.
(26) Wu S.T.; Lackner A.M.; Efron U. *Appl. Opt.* **1987**, *26*, 3441–3445.
(27) Wu S.T.; Wu C.S. *Phys. Rev. A* **1990**, *42*, 2219–2227.
(28) Pauluth D.; Tarumi K. *J. Mater. Chem.* **2004**, *14*, 1219–1227.